An Improved Maximum Likelihood Approach to Image Reconstruction Using Ordered Subsets and Data Subdivisions

Jinhua Sheng and Derong Liu, *Senior Member, IEEE*

***Abstract*—Iterative algorithms such as maximum likelihood expectation maximization (ML-EM) algorithm are rapidly becoming the standard for image reconstruction in emission computed tomography. The maximum likelihood approach provides images with superior noise characteristics compared to conventional filtered backprojection algorithm. A major drawback of the iterative image reconstruction methods is their high computational cost. In this paper, we develop a new algorithm called the improved ordered subset expectation maximization (IOS-EM) algorithm. This algorithm modifies the number of projections in each subset and the step size (i.e., the relaxation factor) for each iteration in order to recover various frequency components in early iteration steps. In the method presented in this paper, the number of projections in a subset increases and the step size decreases after each iteration. In addition, pixel data are grouped into subdivisions to accelerate image reconstruction. Experimental results show that the IOS-EM algorithm can provide high quality reconstructed images at a small number of iterations.**

***Index Terms*—Expectation maximization, filtered backprojection, image reconstruction, iteration algorithms, maximum likelihood, ordered subset.**

I. Introduction

TOMOGRAPHIC image reconstruction has been an active research field in recent years. Soon after the invention of computed tomography (CT) in 1972 [6], reconstruction using filtered backprojection (FBP) was developed for astrophysical applications. Since then, FBP has remained the most widely used reconstruction method in CT. FBP and statistical model based iterative algorithms are the two major classes of reconstruction methods. FBP is widely used in clinical settings for its high speed and easy implementation. Iterative algorithms take into account the statistical nature of the acquired projection data and incorporate the physical model into reconstruction. Typical iterative methods include maximum likelihood approach [15], [16], algebraic reconstruction technology [5], [8], etc.

The well studied maximum likelihood expectation maximization (ML-EM) algorithms have been found to produce very good results in applications. But, it requires a large number of iterations, resulting in delays of the availability of reconstructed images. One of the main reasons for this is that EM algorithms have very slow convergence speed and thus a large number of iterations may be required to obtain an acceptable reconstructed image. Several modifications have been suggested to accelerate the convergence of these algorithms using line search [11] and vector extrapolation [14] techniques. Other fast alternatives have also been proposed to speed up the convergence. One popular and effective method for accelerating reconstruction process involves the use of ordered subset (OS) [7] or block-iterative methods [1]. The ML-EM method combined with the OS algorithm, called the OS-EM method, can accelerate the ML-EM algorithm up to ten times or more. The interest in CT imaging has prompted the development of several ordered subset or block iterative algorithms [3], [9], [13] with the intent of accelerating the iterative reconstruction process.

To improve the convergence speed of existing OS-EM methods and to improve the quality of reconstructed images, we develop in this paper a new method which constitutes a natural extension to the OS-EM algorithm. In Section II of the present paper, we provide some background information about OS-EM algorithms. We then develop, in Section III, an improved OS-EM algorithm. The present algorithm adjusts the number of projections in each subset and the step size for each iteration to recover various frequency components in early steps of iterations. The number of projections in a subset increases and the step size decreases after each iteration. In addition, pixel data will be grouped into subdivisions to accelerate the speed for image reconstruction. Simulation results will be presented in Section IV, where our algorithms will be compared to various existing algorithms including FBP, ML-EM, and OS-EM. We provide a few pertinent remarks in Section V to conclude the present paper.

II. Background

Data in emission CT can be described by the following linear algebraic system [2], [10]

$$Y \sim \text{Poisson}\{CX + R\}$$

where $Y = [y_1, y_2, \ldots, y_M]^T$ is the $M \times 1$ measured projection vector, M is the total number of projections, $X = [x_1, x_2, \ldots, x_N]^T$ is the $N \times 1$ activity image vector, N is the total number of pixels, C is the $M \times N$ response matrix, and R is an $M \times 1$ zero mean random noise vector. Since C consists of the system response for each pixel at each slit ring position for each detector, C will be a very large matrix and is therefore difficult to invert directly. However, C is sparse and iterative methods for computing its inverse become attractive.

Manuscript received May 5, 2003; revised September 11, 2003.

The authors are with the Department of Electrical and Computer Engineering, University of Illinois at Chicago, Chicago, IL 60607 USA (e-mail: jsheng@cil.ece.uic.edu; dliu@ieee.org).

Digital Object Identifier 10.1109/TNS.2003.823015

The measured projection vector Y is Poisson distributed with expected value given by [18]

$$\lambda = E[Y] = CX.$$

In this paper, λ represents the true mean pixel rate of the sinogram and X represents the true mean pixel rate of the image. The ith measurement y_i is an independent Poisson distributed random variable with the mean given by

$$\lambda_i = \sum_{j=1}^{N} c_{ij} x_j$$

where c_{ij} is the ijth element of the response matrix C. The variance of a Poisson distributed random variable is equal to its mean. The variance for each line of response y_i may vary from bin to bin and hence, the noise process may not be stationary. We consider the discretized two-dimensional model. In the above, x_j denotes the expected value of pixel $j, j = 1, \ldots, N$.

Suppose that we count coincidences along M lines. The ith element of the M-dimensional measured projection vector, y_i ($y_i \geq 0$), is the number of coincidences which are counted for the ith line during data collection period. If the image vector is X, the probability of the measurement vector to be Y is

$$P(Y \mid X) = \prod_{i=1}^{M} \left[\frac{\lambda_i^{y_i}}{y_i!} e^{-\lambda_i} \right].$$

The reconstruction problem is to estimate the image vector X given the data measurement Y. As mentioned before, one approach to this problem is the maximum likelihood method which estimates X that maximizes $P(Y \mid X)$ which is equivalent to maximize a log-likelihood function $L(X)$ subject to nonnegative constraints on X, i.e., it finds $X \geq 0$ which maximizes

$$L(X) = \sum_{i=1}^{M} [y_i \log \lambda_i - \lambda_i].$$

The gradient of $L(X)$ is much simpler to compute than that of $P(Y \mid X)$, which is given by

$$\frac{\partial L(X)}{\partial x_j} = \sum_{i=1}^{M} \left[y_i \frac{c_{ij}}{\sum_{l=1}^{N} c_{il} x_l} - c_{ij} \right]. \tag{1}$$

The Kuhn–Tucker conditions for maximizing $L(X)$ subject to nonnegativity constraints [12], [19] are

$$x_j \frac{\partial L(X)}{\partial x_j} = 0 \quad \text{for } j = 1, 2, \ldots, N, \quad \text{if } x_j > 0 \tag{2}$$

and

$$\frac{\partial L(X)}{\partial x_j} \leq 0 \quad \text{for } j = 1, 2, \ldots, N, \quad \text{if } x_j = 0. \tag{3}$$

Conditions (2) and (3) along with the formula given in (1) lead to the maximum likelihood expectation maximization (ML-EM) algorithm

$$\hat{x}_j^{n+1} = \frac{\hat{x}_j^n}{\sum_{i=1}^{M} c_{ij}} \sum_{i=1}^{M} c_{ij} \frac{y_i}{\sum_{l=1}^{N} c_{il} \hat{x}_l^n} \tag{4}$$

where $\hat{x}_j$ is the jth element of the reconstructed image, n is iteration number, i is projection number, and j is the pixel number.

The ML-EM algorithm is a simultaneous updating scheme that has its roots in statistical theory. The update for this algorithm is driven by the likelihood function and has been shown to converge to the most likely solution given the projection data [17]. Even though in general the ML-EM algorithm's convergence rate is quite good, it becomes extremely low for medical images due to their large sizes. Thus, a significant amount of computation is often needed to obtain an acceptable image. The ordered subset method, derived from the ML-EM, consists of applying the ML-EM algorithm to ordered subsets of projections.

III. An Improved Ordered Subset Expectation Maximization Algorithm

The ordered subset (OS) algorithm is a useful method to accelerate image reconstruction for the maximum likelihood expectation maximization (ML-EM) method. The ML-EM method combined with the OS algorithm is called the OS-EM method [7]. With OS-EM, the projection data is grouped into ordered subsets. The OS level is defined as the number of these subsets. The standard ML-EM algorithm is then applied to each of the subsets in turn, using the rows of the response matrix corresponding to these ray sums, i.e., the total number of ray photons which leave the source in the direction of a detector. The resulting reconstruction becomes the starting value for use by the next iteration. In ML-EM algorithm, the nth correction image used for image modification is acquired by a backprojection of λ_i^n which is calculated in all projection views. While in OS-EM algorithm, the correction image is acquired by a backprojection of λ_i^n which is calculated in a subsets of projection views.

The OS-EM algorithm is an ML-EM algorithm acting on a subset S_t of the projections at the time t, which can be written as

$$\hat{x}_j^{n+1} = \frac{\hat{x}_j^n}{\sum_{i=1}^{M} c_{ij}} \sum_{i \in S_t} c_{ij} \frac{y_i}{\sum_{l=1}^{N} c_{il} \hat{x}_l^n}. \tag{5}$$

Subsets S_t in (5) may correspond naturally to groups of projections. In our simulation studies, we use subsets corresponding to projections in opposing pairs, even though other choices may be considered. It is advantageous to select subsets in a balanced way so that pixel activity contributes equally to each subset. The order in which projections are processed is arbitrary, though it may be chosen in a special order. For example, one might encourage substantial new information to be introduced as quickly as possible by choosing first the projection corresponding to the direction with greatest variability in the image, a second projection perpendicular to the first, and third and fourth projections halfway in between the first two, and so on.

To improve the convergence speed of existing OS-EM methods and to improve the quality of reconstructed images, we develop in this paper a new method which constitutes a natural extension to the above OS-EM algorithm. The present algorithm adjusts the number of projections in each subset and the step size for each iteration to recover various frequency

components in early iteration steps. The number of projections in a subset increases and the step size decreases after each iteration.

We note that (4) has an equivalent form as the additive version of the ML-EM algorithm

$$\hat{x}_j^{n+1} = \hat{x}_j^n + \frac{\hat{x}_j^n}{\sum_{i=1}^M c_{ij}} \sum_{i=1}^M c_{ij} \left[\frac{y_i}{\sum_{l=1}^N c_{il}\hat{x}_l^n} - 1 \right]. \quad (6)$$

Our algorithm is developed through analogy observed between the rescaled block iterative EM algorithm [1] and the OS-EM algorithm. Our algorithm updates the current image estimate using only a portion of the projection data, called "subset of projections." This algorithm modifies the number of projections in a subset and the iterative step size after each iteration. The algorithm is given as follows:

$$\hat{x}_j^{n+1} = \hat{x}_j^n + \eta_k \frac{\hat{x}_j^n}{\sum_{i=1}^M c_{ij}} \sum_{i \in S_t} c_{ij} \left[\frac{y_i}{\sum_{l=1}^N c_{il}\hat{x}_l^n} - 1 \right]. \quad (7)$$

The update direction is multiplied by a relaxation factor that differs for each subset and it is computed as $\eta_k = f(t_w, k)$, where k denotes the index of a complete cycle and t_w is a scaling factor. The scaling factor t_w is defined as

$$t_w = \min_j \frac{\sum_{i \in S_t} c_{ij}}{\sum_{i=1}^M c_{ij}}.$$

The function $f(t_w, k)$ above is chosen such that η_k is a sequence of positive numbers (examples follow) and $\eta_k \to 0$ when $k \to \infty$. For the present improved OS-EM (IOS-EM) algorithm, large number of subsets can be used with small relaxation. For example, we choose relaxation factor in our simulation as

$$\eta_k = \eta_0 \frac{t_w}{k^{\frac{1}{4}}} \quad \text{with no noise}$$

and

$$\eta_k = \eta_0 \frac{t_w}{k^{\frac{1}{3}}} \quad \text{with noise.}$$

Generally, η_0 can be chosen as 1. But, η_0 can be chosen smaller, if the number of subsets is larger or the level of noise is higher.

Let the projection data be grouped into T subsets $(S_1, S_2, \ldots, S_T)$, where T is the subset level of projection. In the OS-EM algorithm, the same number of projections are used in each subset $S_1, S_2, \ldots, S_T$. The quality of reconstructed images depends upon the number of projections in a subset. The larger the number of projections in each subset is, the slower the convergence of the reconstructed image will be. In the reconstruction method developed in the present paper, we use (7), and the number of projections in each subset is increased after each iteration step. For example, if the total number of projections in an image is 64, the numbers of subsets can be chosen in successive iterations as 64, 32, 16, 8, 4, 2, and 1, with the corresponding numbers of projections in each subset as 1, 2, 4, 8, 16, 32, and 64, respectively. Such a sequence of subsets implies that the high frequency components are recovered first and the low frequency components are recovered gradually in succeeding iteration steps.

In addition, we will also use the idea of pixel data subdivision in our algorithm. In this case, the pixel data are grouped into subdivisions at intervals of one pixel or several pixels $\{P_1, P_2, \ldots, P_K\}$, where K is the subdivision level of pixels to accelerate image reconstruction and convergence. For example, we can group pixel data into two subdivisions, with one subdivision for even numbered pixels and the other for odd numbered pixels, i.e., we choose $\{P_1, P_2\}$ with $P_1 = (x_1, x_3, \ldots, x_{n-1})$ and $P_2 = (x_2, x_4, \ldots, x_n)$. The modification of the pixels is gradually performed according to different subdivisions.

Finally, our IOS-EM algorithm can be written as follows:

$$\hat{x}_j^{n+1} = \hat{x}_j^n + \eta_k \frac{\hat{x}_j^n}{\sum_{i=1}^M c_{ij}} \sum_{i \in S_t} c_{ij} \left[\frac{y_i}{\sum_{l \in P_k} c_{il}\hat{x}_l^n} - 1 \right], \quad x_j \in P_k, \quad k = 1, 2, \ldots, K. \quad (8)$$

Using this algorithm, the number of projections in each subset is variable to achieve fast convergence and good quality of reconstructed images. For example, the number of projections in a subset can increase as follows for successive iterations: $1 \to 2 \to 4 \to 8 \to 16 \to 32 \to 64$, i.e., the first iteration has 1 projection in each subset, the second iteration has two projections in each subset, and so on. To evaluate the convergence speed and to compare the quality of reconstructed images, we apply the present IOS-EM algorithm (8) to reconstruct images using the following sequences with the total numbers of iterations all equal to 30:

A: $8 \to 8 \to 8 \to 8 \to 8 \to 8 \to 8 \cdots$

B: $1 \to 2 \to 4 \to 8 \to 16 \to 32 \to 64 \cdots$

C: $1 \to 2 \to 2 \to 4 \to 4 \to 4 \to 8$
$\to 8 \to 8 \to 8 \to 16 \to 16 \to 16$
$\to 16 \to 16 \to 32 \to 32 \to 32 \to 32 \to 32 \to 32$
$\to 64 \to 64 \to 64 \to 64 \to 64 \to 64 \to 64 \cdots$

D: $2 \to 2 \to 4 \to 4 \to 4 \to 8 \to 8$
$\to 8 \to 8 \to 16 \to 16 \to 16 \to 16 \to 16$
$\to 32 \to 32 \to 32 \to 32 \to 32 \to 32 \to 64$
$\to 64 \to 64 \to 64 \to 64 \to 64 \to 64 \cdots$

E: $4 \to 4 \to 4 \to 4 \to 8 \to 8$
$\to 8 \to 8 \to 8 \to 16 \to 16 \to 16 \to 16 \to 16$
$\to 16 \to 32 \to 32 \to 32 \to 32 \to 32 \to 32$
$\to 32 \to 64 \to 64 \to 64 \to 64 \to 64 \to 64$
$\to 64 \to 64$

F: $4 \to 8 \to 8 \to 16 \to 16 \to 16$
$\to 32 \to 32 \to 32 \to 32 \to 64 \to 64 \to 64$
$\to 64 \to 64 \cdots$

The first number in each scheme is the number of projections in each subset in the first iteration, the second number is the number of projections in each subset in the second iteration, and so on. We note that the scheme A above is not exactly equivalent to the regular OS-EM algorithms. Though in scheme A, each iteration has the same number of subsets, pixel data subdivision is applied as well to accelerate the convergence. One

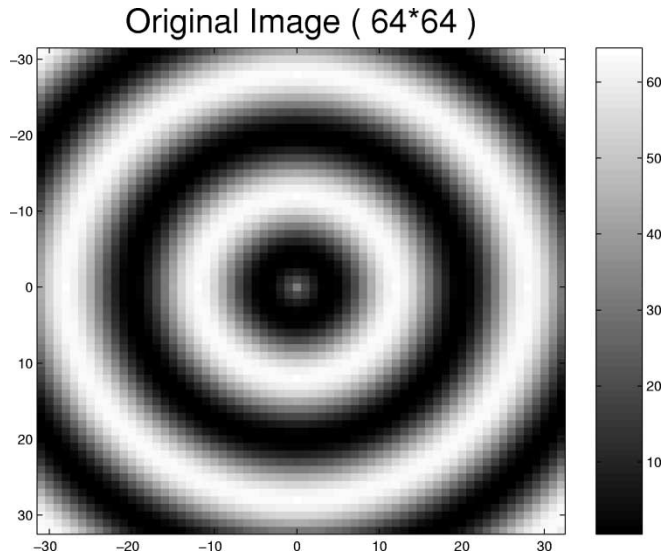

Fig. 1. The original computer generated image.

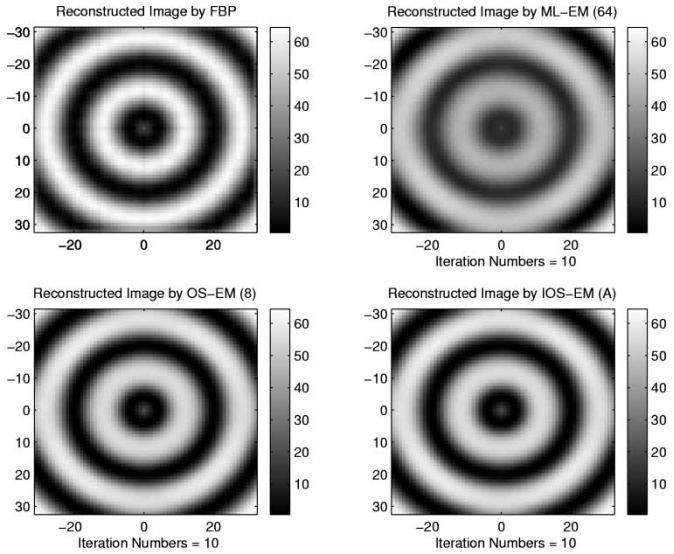

Fig. 2. Images reconstructed from noiseless projection data using FBP, ML-EM, OS-EM, and IOS-EM (scheme A) algorithms.

of the benefits of using our algorithm is to accelerate the recovery of high frequency components of a reconstructed image and to approach the expected value more rapidly, which is difficult when using the ML-EM algorithm. If the number of projections in a subset decreases to one, the algorithms is just like the algebraic reconstruction technique. In this case, reconstructed image is very much influenced by noise in the projection data. Thus, the number of projections in each subset can be increased gradually to reduce the effect of noise. If the number of projections in a subset increases to equal to the total number of views, the algorithm becomes the ML-EM algorithm. In this case, the convergence of the reconstructed image becomes very slow, but reconstructed images are less influenced by noise in the projection data. In summary, the present algorithm is expected to work well for speeding up the convergence and reducing the effect of noise.

IV. Simulation Results

The convergence rate can be measured in terms of the mean absolute error (MAE) and the normalized mean square error (NMSE). The MAE of an image is defined as

$$\mathrm{MAE} = \frac{1}{N}\sum_{j=1}^{N} |\hat{x}_j - \tilde{x}_j|$$

where N is the number of pixels in the object, $\tilde{x}_j$ denotes the value of pixel j of the original image, and $\hat{x}_j$ denotes the value of pixel j of a reconstructed image. The NMSE of an image is defined as

$$\mathrm{NMSE} = \frac{\sum_{j=1}^{N}(\hat{x}_j - \tilde{x}_j)^2}{\sum_{j=1}^{N}\tilde{x}_j^2}.$$

The original computer generated image is shown in Fig. 1. The object array is 64×64 and projections are simulated over 180° with the uniform sampling scheme. Image reconstruction and convergence rate are compared using noiseless projection data (Figs. 2–4) and noisy projection data (Figs. 5–7). The noisy

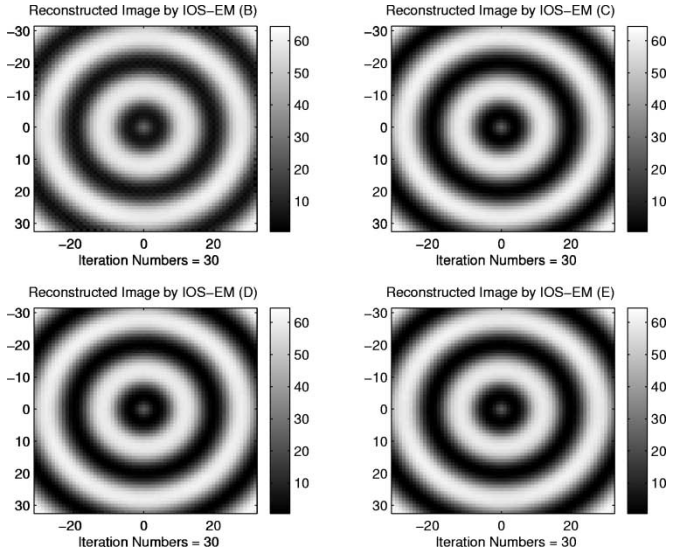

Fig. 3. Images reconstructed from noiseless projection data using schemes B, C, D, and E of the IOS-EM algorithm.

projection data is generated by adding to the original data a uniform field of random coincidences reflecting a scan of 5% of the total counts [4]. Images are reconstructed by using four methods: filtered backprojection (FBP), maximum likelihood expectation maximization (ML-EM), ordered subset-expectation maximization (OS-EM), and improved ordered subset-expectation maximization (IOS-EM) algorithm. Attenuation is not considered in our simulations. In the present IOS-EM algorithm, the pixel data are grouped into two subdivisions. The modification of the pixel is alternately performed based on different subdivisions of pixel. Simple post-reconstruction filtering is used to control the noise. The method ensures that the iterative algorithms converge toward a uniform resolution. The convergence rate is measured by MAE and NMSE.

Images reconstructed by FBP, ML-EM, OS-EM, and IOS-EM (scheme A) algorithms are shown in Fig. 2. In IOS-EM algorithm using scheme A, the number of projections in each subset

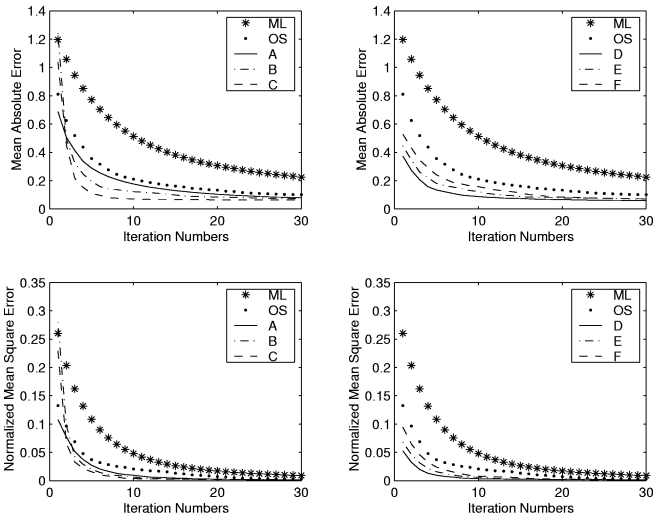

Fig. 4. The mean absolute error and the normalized mean square error for ML-EM, OS-EM, and various schemes of the IOS-EM algorithm for reconstruction from noiseless projection data.

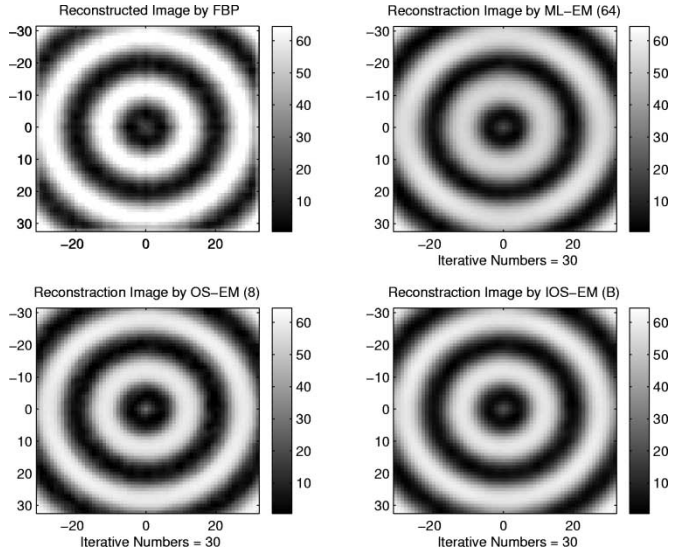

Fig. 5. Images reconstructed from noisy projection data using FBP, ML-EM, OS-EM, and IOS-EM (scheme B) algorithms.

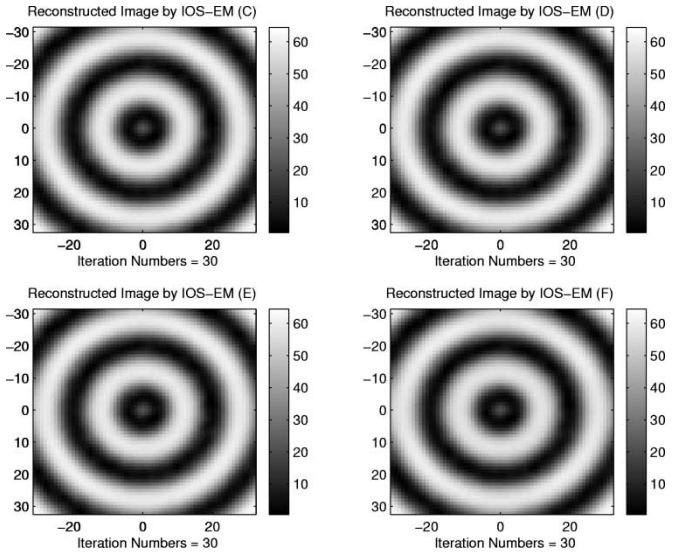

Fig. 6. Images reconstructed from noisy projection data using schemes C, D, E, and F of the IOS-EM algorithm.

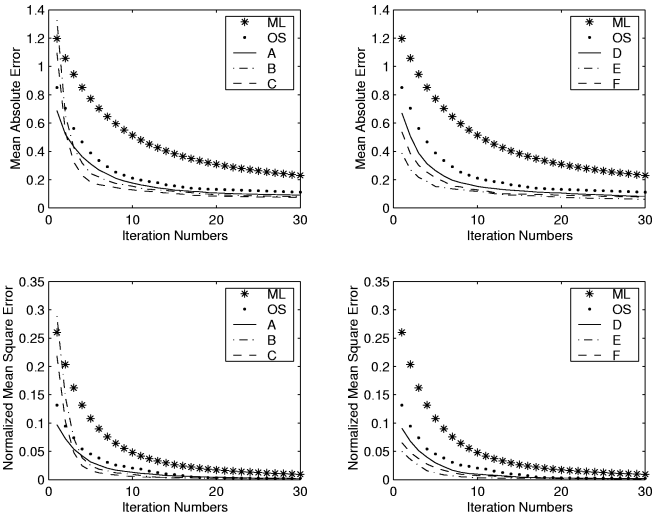

Fig. 7. The mean absolute error and the normalized mean square error for ML-EM, OS-EM, and various schemes of the IOS-EM algorithm for reconstruction from noisy projection data.

is kept fixed at 8. It is therefore expected that other schemes will perform better than scheme A, as is shown in Fig. 3 using schemes B, C, D, and E. The MAE and the NMSE for various ML-EM, OS-EM, and IOS-EM algorithms are shown in Fig. 4. From Fig. 4, we see that scheme C performs the best since it has the fastest convergence. Under the conditions of these simulations, the algorithm we developed in this paper appears to have faster convergence than ML-EM and OS-EM algorithms.

To confirm that the behavior of the various preconditioners are not different under noisy conditions, simulations are also performed using noisy projection data. Reconstructed images using FBP, ML-EM, OS-EM, and IOS-EM (scheme B) are shown in Fig. 5, and reconstructed images using schemes C, D, E, and F of IOS-EM are shown in Fig. 6. The convergence rate compared with all kinds of reconstruction algorithms using noisy projection data are shown in Fig. 7. From Fig. 7, we see that scheme E has the fastest convergence speed. Again, the algorithm we developed in this paper has faster convergence than ML-EM and OS-EM algorithms.

V. Conclusion

Iterative image reconstruction methods such as maximum likelihood expectation maximization (ML-EM) algorithm and algebraic reconstruction technology, have several advantages over analytical image reconstruction methods such as filtered backprojection. The major drawback with the iterative image reconstruction is the computational cost, that is, the slow convergence speed of the reconstructed image. This is one of the reasons that the iterative method has never been used in clinical applications. To reduce computation time, an ordered subsets (OS) algorithm was introduced. In this method, the projection data are grouped into subsets and the modification of the pixels in a reconstructed image is performed by using the projection data in one subset at a time. The OS algorithm

can accelerate the recovery of high frequency components of a reconstructed image, which is difficult to obtain when using ML-EM algorithm. If the number of projections in a subset increases to equal to the total number of views, the algorithm becomes the ML-EM algorithm. In this case, the high frequency components are difficult to recover. On the other hand, if the number of projections in a subset is reduced to one, the algorithm is just like the algebraic reconstruction technique. In this case, reconstructed images are very much influenced by noise in the projection data. The appropriate choice of subset level depends on a number of factors, for example, subset balance and the level of noise in the projection data. Generally speaking, it is better not to use less than four projections per subset. OS-EM algorithm requires more projections per subset to converge if the level of noise in the projection data is high.

The quality of reconstructed images depends upon the number of projections in a subset. We developed a new algorithm to reconstruct high quality images with fewer number of iterations. The scheme of the proposed algorithm is to increase the number of projections per subset after each step of iteration. In addition, based on the idea of data subdivision, pixel data are also grouped into subdivisions to accelerate image reconstruction. The experimental results show that the present IOS-EM algorithm can provide high quality reconstructed images at a small number of iterations. Scheme C is superior to other schemes for projections without noise, and scheme E is recommended for projections with Poisson noise.

REFERENCES

[1] C. L. Byrne, "Block-iterative methods for image reconstruction from projections," *IEEE Trans. Image Processing*, vol. 5, pp. 792–794, May 1996.

[2] G. Chinn and S.-C. Huang, "A general class of preconditioners for statistical iterative reconstruction of emission computed tomography," *IEEE Trans. Med. Imaging*, vol. 16, pp. 1–10, Feb. 1997.

[3] H. Erdoğan and J. A. Fessler, "Ordered subsets algorithms for transmission tomography," *Phys. Med. Biol.*, vol. 44, no. 11, pp. 2835–2851, 1999.

[4] J. A. Fessler and A. O. Hero, "Space-alternating generalized expectation-maximization algorithm," *IEEE Trans. Signal Processing*, vol. 42, pp. 2664–2677, Oct. 1994.

[5] R. Gordon, R. Bender, and G. T. Herman, "Algebraic reconstruction techniques (ART) for three-dimensional electron microscopy and x-ray photography," *J. Theoret. Biol.*, vol. 29, no. 3, pp. 471–481, 1970.

[6] G. N. Hounsfield, "Computerized transverse axial scanning (tomography): Part 1. Description of system," *Brit. J. Radiol.*, vol. 46, no. 552, pp. 1016–1022, 1973.

[7] H. M. Hudson and R. S. Larkin, "Accelerated image reconstruction using ordered subsets of projection data," *IEEE Trans. Med. Imaging*, vol. 13, pp. 601–609, Dec. 1994.

[8] G. T. Herman, *Image Reconstruction From Projections: The Fundamentals of Computerized Tomography*. New York: Academic, 1980.

[9] C. Kamphuis and F. J. Beekman, "Accelerated iterative transmission CT reconstruction using an ordered subsets convex algorithm," *IEEE Trans. Med. Imaging*, vol. 17, pp. 1101–1105, Dec. 1998.

[10] K. Lange and R. Carson, "EM reconstruction algorithms for emission and transmission tomography," *J. Comput. Assist. Tomogr.*, vol. 8, no. 2, pp. 306–316, 1984.

[11] R. M. Lewitt and G. Muehllehner, "Accelerated iterative reconstruction for positron emission tomography based on the EM algorithm for maximum likelihood estimation," *IEEE Trans. Med. Imaging*, vol. MI-5, pp. 16–22, Mar. 1986.

[12] D. Luenberger, *Linear and Nonlinear Programming*. Reading, MA: Addison-Wesley, 1984.

[13] S. H. Manglos, G. M. Gagne, A. Krol, F. D. Thomas, and R. Narayanaswamy, "Transmission maximum likelihood reconstruction with ordered subsets for core beam CT," *Phys. Med. Biol.*, vol. 40, no. 7, pp. 1225–1241, 1995.

[14] N. Rajeevan, K. Rajgopal, and G. Krishna, "Vector-extrapolated fast maximum likelihood estimation algorithms for emission tomography," *IEEE Trans. Med. Imaging*, vol. 11, pp. 9–20, Mar. 1992.

[15] A. J. Rockmore and A. Macovski, "A maximum likelihood approach to emission image reconstruction from projections," *IEEE Trans. Nucl. Sci.*, vol. NS-23, pp. 1428–1432, Aug. 1976.

[16] L. A. Shepp and Y. Vardi, "Maximum likelihood reconstruction for emission tomography," *IEEE Trans. Med. Imaging*, vol. MI-1, pp. 113–122, Oct. 1982.

[17] J. A. Stamos, W. L. Rogers, N. H. Clinthorne, and K. F. Koral, "Object-dependent performance comparison of two iterative reconstruction algorithms," *IEEE Trans. Nucl. Sci.*, vol. 35, pp. 611–614, Feb. 1988.

[18] Y. Vardi, L. A. Shepp, and L. Kaufman, "A statistical model for positron emission tomography," *J. Amer. Statist. Assoc.*, vol. 80, no. 389, pp. 8–37, 1985.

[19] E. Veklerov, "How to compute the difference between tomographic images," *IEEE Trans. Med. Imaging*, vol. 13, pp. 566–569, Sept. 1994.